Environ. Sci. Technol. 1992, 26, 896–901

66/79350

Dissolution of Dense Chlorinated Solvents into Groundwater. 2. Source Functions for Pools of Solvent

Richard L. Johnson* and James F. Pankow

Department of Environmental Science and Engineering, Oregon Graduate Institute, 19600 N. W. von Neumann Drive, Beaverton, Oregon 97006-1999

■ When a spill of dense chlorinated hydrocarbon (CHC) solvent occurs into the subsurface, penetration into the saturated zone is likely to lead to the accumulation of pools of solvent on the tops of low-permeability layers. Steady-state dissolution from such pools was modeled. The dissolution rate depends on the molecular diffusion coefficient, the vertical dispersivity α_v, the groundwater velocity $\bar{v}$, the solubility, and the pool length. A value for α_v for dissolution of trichloroethylene in a sand-filled physical model was found to be ~0.000 23 m. This is consistent with vertical dispersivities reported from field experiments in heterogeneous media. With α_v = 0.000 23 m, at typical groundwater velocities, dissolution from CHC pools was found to be very slow; pools containing a few hundred to a few thousand kilograms of CHC solvent will persist for decades to centuries. Pool lifetimes can be shortened by increasing the groundwater velocity through pumping. However, lifetimes will not usually be reduced by more than a factor of 5. Even after a pool has totally dissolved away, contaminants may remain within the aquitard on which the pool originally formed. The release into the aquifer of CHC solvents dissolved in the pores of the aquitard can persist at a significant rate for many years. The implication of these results is that, for many sites contaminated with CHC solvents, the focus of remediation may need to be on long-term control as opposed to attempts at "quick fixes".

Introduction

Spills of dense chlorinated hydrocarbon (CHC) solvents are widely recognized as common causes of groundwater contamination. Relatively small releases of CHC solvents such as trichloroethylene (TCE) can produce substantial and long-lasting sources of groundwater contamination. This is due in large part to their physical properties. Specifically, their high densities and low viscosities allow them to sink into aquifers. Once in the groundwater zone, their solubilities are sufficiently high to cause significant contamination and little retardation, but also sufficiently low to result in persistent sources.

The subsurface behavior of CHC solvents has been examined from both physical and mathematical viewpoints (*1–6*). This prior work has shown that, in porous media, penetration of the capillary fringe by a given CHC solvent can only occur when the pressure head of the CHC accumulated at the capillary fringe has become sufficiently large. In other words, the density difference between the CHC and water is not, by itself, sufficient to cause penetration. The pressure head required for penetration increases as the grain size of the medium decreases.

Once penetration of the capillary fringe occurs, downward movement will continue until all of the CHC solvent is present as suspended fingers (ganglia) in the porous medium and/or as pools of CHC perched on lower-permeability zones. Once a pool starts to form on the top of a low-permeability layer somewhere above the bottom of the aquifer, a continued supply of CHC will cause (1) enlargement of the pool, (2) penetration of the layer, and/or (3) spawning of new downward-moving fingers at the perimeter of the layer. Because fingers tend to have small dimensions in the saturated zone, and because a significant downward flow of CHC can occur through a finger with a very small cross section, a significant fraction of the CHC mass in the saturated zone may be present as pools. For a large spill, a pool on the aquitard defining the bottom of the aquifer may contain most of the spilled CHC. Such a pool could be relatively uniform in thickness, but a pool of variable thickness is probably more likely due to unevenness or inclination(s) in the interface between the aquifer and the aquitard.

No field-scale experiments have yet been reported that examine the CHC penetration process in natural, heterogeneous media. Therefore, the sizes, shapes, and distributions of the CHC fingers that can develop in typical saturated zones following a large spill remain subject to considerable speculation. In the field, actual liquid CHC has been found in the saturated zone at only a few spill sites. At one such site, tri- and perchloroethylene (TCE and PCE) were found in an aquifer beneath an industrial facility (*7*). Although liquid-phase CHCs were found in wells over an irregularly shaped area measuring roughly 600 m by 600 m, neither the size(s) nor shape(s) of the CHC source zone(s) could be determined.

Because CHC trapped as fingers is relatively dispersed within the porous medium, contact between the groundwater and the CHC results in concentrations leaving the fingers which are at or near saturation values (*3*). In contrast, pools perched on lower-permeability zones have very low profiles with respect to the flowing groundwater, and contact between the pool and the groundwater is limited. As a result, dissolution from a pool surface will be controlled by vertical dispersion. Because many CHCs have limited solubilities, the rate of dissolution is likely to be low, and substantial times may be required to completely dissolve the pool. Thus, in a spill morphology that involves both fingers and pools, it will generally take substantially longer to dissolve the pools than to dissolve the fingers. It is therefore important to understand the factors which control the rate of dissolution from CHC solvent pools. Despite this importance, comparatively little attention has yet been given to obtaining quantitative estimates of pool source strengths in the saturated zone. The purpose of this paper is to address this issue.

Theory

Schwille (*1*) conducted a series of physical-model experiments examining the dissolution of pools of TCE and 1,1,1-trichloroethane (TCA). The experimental setup used is shown schematically in Figure 1. The physical model was 1.5 m long by 0.5 m wide by 0.25 m deep. The groundwater velocity was varied between 0.45 and 2.7 m/day, and the hydraulic conductivity of the sand was 0.0035 m/s. The volume-averaged concentrations of TCE or TCA in the overall tank effluent were reported by Schwille and have been used here to calculate a *surface-area-averaged* mass-transfer rate M_a (g m^{-2} day^{-1}). The boundary conditions approximated by the model are given in Figure 1. The value of M_a will depend on (1) the sol-

 0013-936X/92/0926-0896$03.00/0 © 1992 American Chemical Society

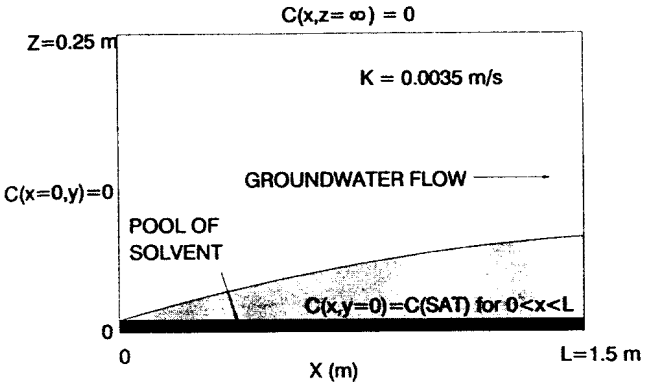


Figure 1. Schematic drawing showing Schwille's (*1*) dissolution experiment setup and boundary conditions.

ubility of the solvent, (2) the groundwater velocity, (3) the length of the pool, and (4) the vertical dispersion coefficient. Since the first three are known for Schwille's (*1*) work, the vertical dispersion coefficient for that case can be estimated using the measured M_a values.

As noted above, the dissolution process will be controlled by the vertical dispersion of dissolved solvent up and away from the pool. The vertical dispersion coefficient (D_v) is often treated as a combination of molecular diffusion and mechanical dispersion (*8*):

$$D_v = D_e + \bar{v}\alpha_v \tag{1}$$

where D_e is the effective aqueous diffusion coefficient (m^2/s) in the porous medium, α_v is the vertical transverse dispersivity (m), and $\bar{v}$ is the average groundwater velocity.

Values of D_e are typically on the order of 10^{-10} m^2/s. For example, a D_e value for TCE at 20 °C of 2.7×10^{-10} m^2/s has been reported by Hunt et al. (*9*). Transport by diffusion can be retarded substantially if the solute of interest partitions strongly to the soil matrix. However, sorption does not affect diffusive transport at steady state, for which the concentration gradient in the aqueous phase remains constant.

Because the times required for total pool dissolution are generally exceedingly long in comparison with the contact time between the pool and the flowing groundwater, it is appropriate to model the dissolution process using a steady-state form of the advection–dispersion equation. Also, because the pools are generally wide in comparison to the horizontal transverse mixing process, a two-dimensional form of the equation can be used:

$$\bar{v}\frac{\partial C}{\partial x} = D_v\frac{\partial^2 C}{\partial z^2} \tag{2}$$

Because sorption is not important at steady state, and because D_e is not strongly dependent upon the molecular size or the properties of the porous medium, values of D_e in the range $1–5 \times 10^{-10}$ m^2/s are applicable for a wide range of CHC solvents and porous media. This makes it possible to estimate solvent dissolution behavior over a wide range of subsurface conditions and contaminant types.

Field and laboratory studies suggest that vertical transverse dispersion in groundwater systems is generally a weak process. At low groundwater velocities (e.g., 0.1 m/day) vertical dispersion is on the order of molecular diffusion (even in heterogeneous aquifers) and does not appear to be scale dependent (*10*, *11*). In laboratory experiments, transverse dispersivities are frequently observed to be on the order of 1 mm or less. For example, Anderson (2) conducted experiments in a three-dimensional tank (1 m high × 0.75 m wide × 1 m long) in which horizontal transverse dispersivities of $\sim 3 \times 10^{-4}$ m were observed. Thus, molecular diffusion can play a significant role in dissolution from pools, and the mechanical dispersion component is expected to dominate only when velocities are greater than 0.1 m/day.

Hunt et al. (*9*) presented an analytical solution of eq 1 for the boundary conditions $C(x,y=\infty) = 0$, $C(x=0,y) = 0$ and $C(x,y=0) = C_{SAT}$ for $0 < x < L_p$, where L_p is the length of the pool in the direction of groundwater flow. Under these conditions, the vertical concentration profile at the downgradient edge of the pool ($x = L_p$) is then given by

$$C(L_p,z) = C_{SAT}\,\mathrm{erfc}\left(\frac{z}{2(D_vL_p/\bar{v})^{1/2}}\right) \tag{3}$$

where C_{SAT} is the saturation concentration of the compound of interest. The elevation of the pool surface is taken as $z = 0$, with z measured positively upward. If the geometry of the pool is approximated as a rectangle, the nature of the vertical concentration profile at the downgradient edge of the pool will determine the value of M_a. Within the context of the assumptions made above, the width of a rectangular pool will not affect M_a. The value of M_a will be given by

$$M_a = \frac{\bar{v}\theta}{L_p}\int_0^\infty C(L_p,z)\,dz \tag{4}$$

where θ is the porosity of the medium. The integrated form of eq 4 is given by Bird et al. (*12*) and can be expressed as

$$M_a = C_{SAT}\theta\sqrt{4D_v\bar{v}/\pi L_p} \tag{5}$$

Essentially no field information is available on the geometry of pools. However, Schwille's (*1*) physical-model work can again provide some guidance in this regard. For example, in his large two-dimensional trough experiments with coarse sand, a 0.024-m^3 spill of tetrachloroethylene (i.e., perchloroethylene, PCE) was released. Approximately 0.016 m^3 of solvent reached the bottom of the model and produced a pool that was ~5 m long with an average thickness of ~0.04 m. Although it is expected that the pools will tend to be thicker and shorter in finer grained media (due to increased capillary forces), for the following calculations a uniform length/thickness ratio of 100 will be assumed. It will also be assumed that all of the pore space within the pool is filled with CHC. This will likely overestimate the mass contained within a pool, though not by more than a factor of 2.

Equations 3–5 assume that the porous medium is isotropic. The modeling discussion in the following section also assumes this to be the case. This does not represent a major limitation to the approach presented here because the relationship between pools and aquifer heterogeneities has been implicitly taken into account. For example, the pools discussed here are assumed to have formed at boundaries between zones of different permeability (e.g., a less-permeable layer underlying a more-permeable one). In this case, the lateral extent of a pool on a low-permeability layer would be expected to be equal to or less than the horizontal length of the layer. Moreover, the lateral extent of the more-permeable zone overlying the pool will also tend to be greater than the length of the pool. In addition, pools tend to be vertically quite thin, and the "dissolution zone" above the pool is also very thin (e.g., a few centimeters). Thus, in many cases the thickness of the dissolution zone will be less than the vertical scale of

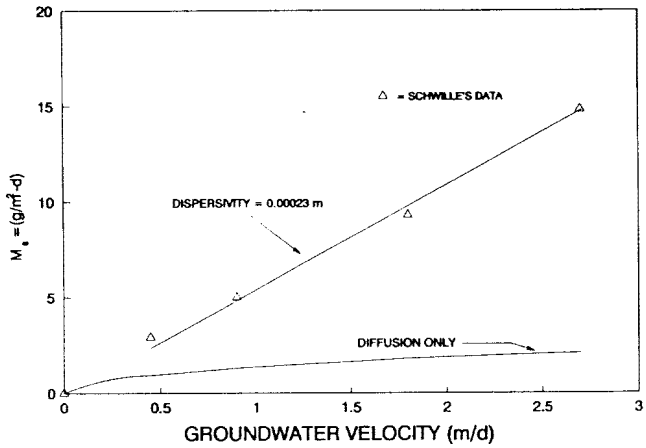


Figure 2. Data from Schwille's (*1*) dissolution experiments and results of simulations using eq 3.

Table I. Mass-Transfer Coefficient and Dispersivity Data Calculated from Data of Schwille (*1*)

velocity, m/day	mass-transfer coefficient, g m^{-2} day^{-1}	calculated dispersivity, m
0.45	2.9	0.000 29
0.9	4.3, 5.6	0.000 25
1.8	9.3	0.000 22
2.7	14.8	0.000 25

heterogeneities, and as a result the aquifer in that zone is likely to be relatively homogeneous.

Modeling

The input values we have selected for modeling are representative of what might be expected for sandy aquifers at both the laboratory and field scales. It may be appropriate at some sites to select other values. The dispersivity values are consistent with recent data from field studies in heterogeneous media.

Determination of α_v from TCE Pool Dissolution Data of Schwille. The values of M_a based on Schwille's (*1*) data for the dissolution of a pool of TCE are given in Table I and Figure 2. As expected based on eq 1, the results indicate that M_a increases with increasing groundwater velocity. The value of α_v that gives the measured value of M_a for each velocity used by Schwille (*1*) was determined using eq 1 with $D_e = 2.7 \times 10^{-10}$ m^2/s together with eqs 3 and 4 and a C_{SAT} for TCE of 1100 g/m^3 (=1100 mg/L) at 20 °C. The results indicate an average α_v of approximately 0.000 23 m. Figure 2 compares the dependence of M_a on $\bar{v}$ for α_v = 0.000 23 m with the Schwille TCE data. This dispersivity is consistent with the microscale transverse dispersivities of 0.0002–0.0004 m measured by Anderson (*2*) for PCE in a similar sand.

M_a as a Function of Pool Length. By use of $D_e = 2.7 \times 10^{-10}$ m^2/s together with the value for α_v of 0.000 23 m determined above for relatively coarse sand, values of M_a as a function of pool length L_p and groundwater velocity $\bar{v}$ were obtained using eqs 3 and 4. When interpreted using the left scale of the y-axis, the results in Figure 3 pertain to the compound TCE (C_{SAT} = 1100 g/m^3 at 20 °C). Because both α_v and D_e will be fairly constant from solvent to solvent, the results in Figure 3 can be generalized. In particular, when interpreted using the right scale of the y-axis, the results pertain to a hypothetical solvent with unit solubility (i.e., 1 g/m^3). Figure 3 can thus be applied to any solvent of interest by multiplying the values on the right scale of the y-axis by the solubility of that solvent. For example, for methylene chloride, which has a solubility

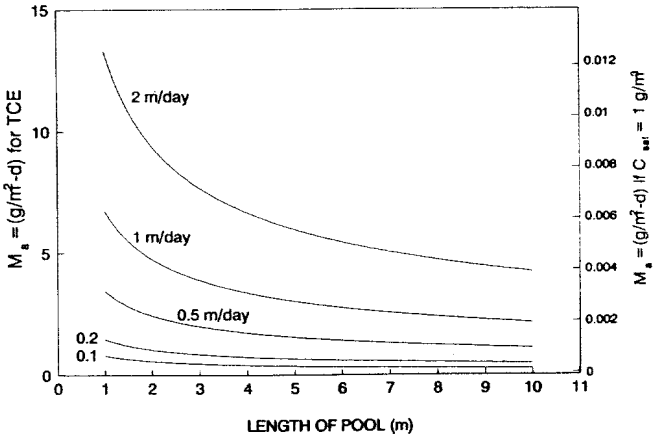


Figure 3. Mass-transfer rate data as a function of pool length for several velocities. The left-hand axis applies for TCE. The right-hand axis applies for any compound after being multiplied by the compound's solubility.

of 20 000 g/m^3 at 20 °C, the right scale of the y-axis would extend from 0 to 240. A pool of methylene chloride will therefore dissolve away much more quickly than will a similar pool of TCE. Multiplying the right scale of the y-axis by C_{SAT} for TCE returns the left scale of the y-axis.

The trend of decreasing M_a with increasing pool length may be understood as follows. As the length of the pool in the direction of flow increases, the hydraulic residence time above the pool will increase proportionally. However, as the water moves across the top of the pool, the concentration gradient at the water/pool interface decreases and so the instantaneous dissolution rate also decreases. Thus, since M_a is the pool surface-area-averaged mass-transfer rate in units of grams per square meter per day, the value of M_a decreases as the length of the pool increases.

Time for Complete Pool Dissolution. To calculate the time required for the complete dissolution of a pool of solvent, we require both the pool geometry and the value of M_a for the pool. If we assume a pool of constant thickness with a length/thickness ratio of 100, and that the pool may be approximated as a rectangle, then the mass of solvent in a pool will be given by

$$\text{mass of CHC} = 0.01 L_p^3 \theta \rho \qquad (6)$$

where θ is the porosity and ρ is the density of the solvent. We will take θ = 0.35 and $\rho = 1.6 \times 10^6$ g/m^3 for these calculations.

Assuming that the areal dimensions of the pool do not change during the course of the dissolution process, i.e., that dissolution just leads to a thinning of the pool (this assumption will be evaluated below), the time to complete dissolution τ_p (years) will be given by

$$\tau_p = 0.01 L_p \theta \rho / 365 M_a \qquad (7)$$

Using eq 5 to substitute for M_a, we obtain

$$\tau_p = 2.43 \times 10^{-5} \rho C_{SAT}^{-1} \sqrt{L_p^3 / D_v \bar{v}} \qquad (8)$$

Figure 4 illustrates how the lifetime τ_p varies as a function of groundwater velocity for various values of L_p. Increasing L_p by a factor of 2 increases τ_p by a factor of almost 3. Clearly, at typical groundwater velocities (e.g., 0.1–0.3 m/day), spills of only a few hundred liters will persist for tens to hundreds of years. Even if groundwater velocities are increased substantially during pump-and-treat remediation, it is unlikely that dissolution times can be reduced by more than a factor of 5. As can be seen in eq 8, a factor

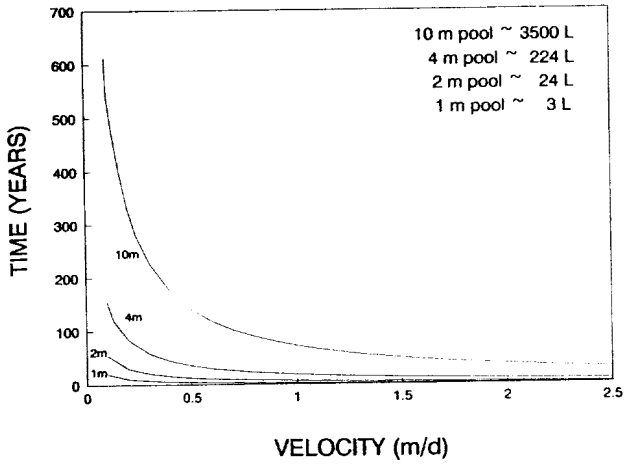


Figure 4. Dissolution time versus groundwater velocity for TCE for four pool lengths.

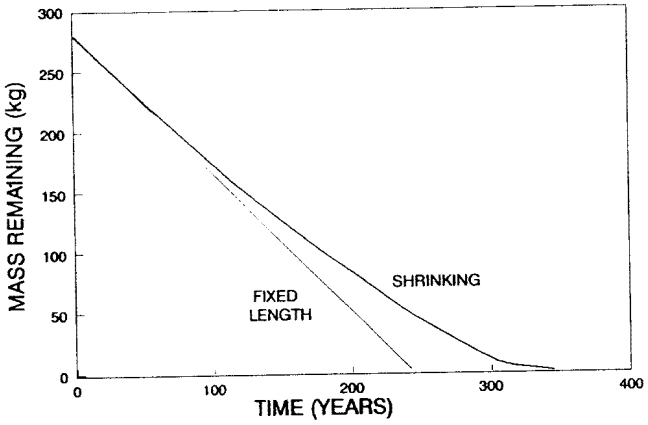


Figure 5. Mass removed from a 10-m pool of TCE as a function of time for a pool of fixed length and a pool which shrinks with time ($\bar{v}$ = 0.3 m/day).

of 25 increase in velocity would be required to achieve a factor of 5 decrease in dissolution time.

Evaluation of Constant Pool Length and Uniform Pool Thickness Assumptions. Dissolution will occur most rapidly at the upgradient edge of a pool where the concentration gradient is the steepest. We also note that most pools will tend to be thinnest along their edges. Both of these factors will cause the length of a pool to decrease as dissolution proceeds. As noted above, eqs 7 and 8 assume that during dissolution the length of the pool remains constant and the thickness of the pool decreases uniformly. Thus, eqs 7 and 8 assume that the location of the upgradient and downgradient edges of the pool remain constant at $x = 0$ and $x = L_p$. For a given mass of solvent in a pool, eqs 7 and 8 will therefore underestimate the time required for complete dissolution. To assess the degree of underestimation, a two-dimensional compartmental model was developed. The model was applied to a pool whose initial length was taken to be 10 m. The thickness of the pool was not assumed to be constant at 0.01 L_p, but rather was assumed to increase from zero at the up- and downgradient edges to 0.2 m at the center. The groundwater velocity was taken as 0.3 m/day.

The 10-m length of the pool was divided up into 10 compartments of 1 m each. A mass-transfer rate for each compartment was determined according to its distance from the upgradient edge. For example, the mass-transfer rate for the first 1-m compartment was computed normally using eq 5 with L_p = 1 m; the mass-transfer rate for the second compartment was computed as $2M_a$ for a 2-m pool minus the M_a for a 1-m pool; and, the mass-transfer rate for the third compartment was computed as $3M_a$ for a 3-m pool minus $2M_a$ for a 2-m pool. (It should be remembered that M_a is a surface-area-averaged mass-transfer rate.) As the mass in each compartment was brought to zero, dissolution from that compartment was halted and the M_a values for the remaining compartments were adjusted appropriately.

As can be seen in Figure 5, at early times, dissolution occurs at nearly the same rate as computed using eqs 7 and 8 with L_p constant. As the pool shrinks, however, the overall dissolution rate decreases and the rate of removal slows. Nevertheless, for this example, the overall time to dissolution is only increased by about 40%. Thus, the fixed-length solution represented by eqs 7 and 8 and the results presented in Figure 4 for TCE are good approximations.

Diffusion In/Out of an Aquitard Underlying a Pool. In addition to dissolving into the groundwater flowing above it, the solvent in a pool can move into an aquitard (or simply a lower permeability layer) beneath it. This can occur either when the solvent phase penetrates into the pores beneath the pool or when molecular diffusion carries the dissolved solvent into the pore water beneath the pool.

Johnson et al. (*13*) have shown that molecular diffusion can be an important transport mechanism even when contaminants have been in contact with an aquitard for only a few years. If, as is the case at many contaminated sites, the solvent has been in contact with the aquitard for several decades, then a substantial mass of solvent will have entered it by diffusion. If the solvent pool is eventually removed by dissolution (or direct pumping) from the top of the layer, then diffusion will begin to carry the solvent back into the aquifer. Under these conditions, removal of the CHC from the aquitard will be a very slow process, requiring many decades to accomplish.

Diffusion of the solvent into and out of the aquitard can be simulated with a one-dimensional representation of Fick's second law:

$$R \frac{\partial C}{\partial t} = D_e \frac{\partial^2 C}{\partial z^2} \tag{9}$$

where R is the retardation coefficient. During the period in which diffusion is occurring into the aquitard, the source at the top may be assumed to be constant at the saturation concentration of the solvent. If it can be assumed that the aquitard is infinitely thick and the groundwater velocity within the aquitard is zero, then the solution to eq 9 for the initial and boundary conditions $C(z) = 0$ at $t = 0$ and $C(z=0) = C_{SAT}$ at $t > 0$ is the familiar one given by Crank (*14*):

$$\frac{C}{C_0} = \text{erfc} \frac{x}{2\sqrt{D_e t/R}} \tag{10}$$

Once the overlying pool has been removed, it will be assumed that the concentration in the aquifer at the top of the aquitard is effectively zero. The moving groundwater will not, of course, be able to maintain an exactly zero concentration at the interface between the aquifer and the aquitard. Nevertheless, the assumption of a zero-concentration boundary condition at the interface will lead to lower-bound estimates of the time required to reduce the flux of solvent from the aquitard to acceptable levels. At the same time, an upper-bound estimate of the volume of groundwater that can be contaminated at problematic levels per day by the solvent diffusing from the aquitard

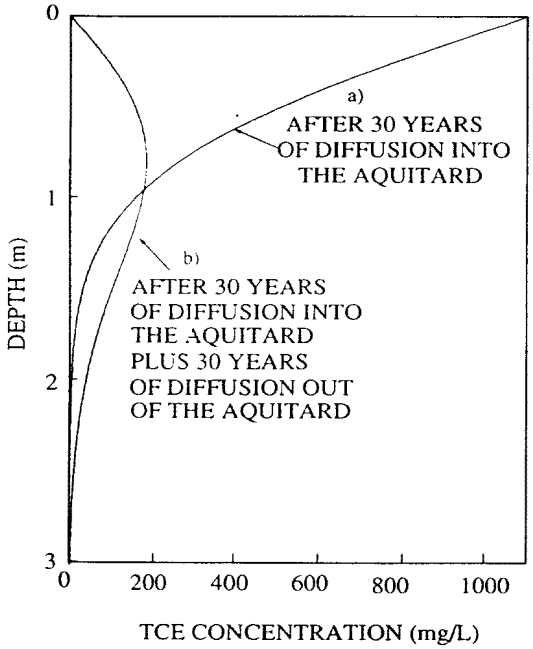


Figure 6. Concentration profiles at the time of removal of a 30-year-old pool and after an additional 30 years of pumping.

can be estimated by taking the product of the mass flux and L_p^2 and dividing by the drinking water limit of the contaminant of interest.

The flux from the aquitard can be estimated using Fick's first law:

$$F = -D_e\theta \left.\frac{\partial C}{\partial z}\right|_{\text{interface}} \qquad (11)$$

where the concentration C is that in the pores of the aquitard and the gradient is evaluated at the aquifer/aquitard interface. For the case of TCE, the initial flux will be on the order of 0.1 g m^{-2} day^{-1}. Over time this will drop, such that after 30 years it will be ~0.003 g m^{-2} day^{-1}. Although this is considerably less than the mass-transfer rate from the original pool, as the following example shows, it can still lead to substantial groundwater contamination.

Consider the case of a rectangular pool of solvent for which L_p = 10 m. According to eq 5, such a pool might contain about 5000 kg of solvent. Assuming that the pool persisted on the top of the aquitard for 30 years, and if sorption within the aquitard was not important (R = 1), then the diffusion of the solvent into the aquitard would have a profile similar to curve a in Figure 6. The mass of TCE in the aquitard would be ~17.5 kg. If the pool were removed after 30 years and assuming a subsequent zero-concentration boundary condition at the interface, then the rate at which groundwater could become contaminated at the drinking water limit of 5 μg/L (e.g., for TCE) would initially be ~2 000 000 L/day.

After 30 years of natural or induced flushing above the aquitard, the concentration profile in the aquitard would look similar to curve b in Figure 6. At this point, ~42% of the mass initially carried into the aquitard would remain there. The rate at which groundwater could be contaminated at the drinking water limit would now drop to ~60 000 L/day. If the groundwater velocity is decreased (e.g., pumping is stopped), then groundwater concentrations above the aquitard would increase.

If the contaminant sorbed to the soil matrix (e.g., R = 4), then after 30 years the depth of penetration would be less than that shown in Figure 6. However, the total mass which would have been carried into the aquitard would be greater. In addition, after 30 years of diffusion back into the aquifer, on the order of 85% of the mass would remain in the aquifer.

Conclusions

The rate at which a pool of CHC solvent dissolves will depend on the vertical dispersivity α_v, the groundwater velocity, $\bar{v}$, the solubility C_{SAT}, and the length of the pool. Data from the laboratory experiments of Schwille (*1*) and others suggests that α_v values for CHC solvents are on the order of 10^{-3}–10^{-4} m in medium to coarse sand. Due to this limited dispersion, at typical groundwater velocities, dissolution from pools of CHC solvents will be very slow. Consequently, for pools containing a few hundred to a few thousand kilograms of CHC solvent, dissolution times will be on the order of decades to centuries. If groundwater velocities are increased (e.g., by pumping), then removal times can be reduced. However, with such techniques, it can be difficult to (1) maintain high velocities under radial flow conditions at significant distances from the pumping well, (2) obtain enough water from the aquifer to maintain high velocities, and (3) deal with the large volumes of contaminated water produced. Moreover, even at $\bar{v}$ = 2 m/day, a pool containing ~6000 kg of solvent may be expected to last 50 years or more. Enhancement of the water solubility of the solvent (e.g., with a micelle-forming surfactant) will accelerate the removal.

Even when a pool has been totally dissolved away, there is a strong possibility that contaminants will remain within the aquitard or low-permeability layer on which the pool originally formed. This can occur because the CHCs entered the aquitard either as a separate phase or as the result of molecular diffusion in the aqueous phase. In either case, hundreds of grams per square meter can be retained in the aquitard. This material will slowly diffuse out of the aquitard and can result in the contamination of hundreds of thousands of liters of groundwater per day for many decades.

We conclude that even under optimum conditions (e.g., homogeneous media, uniform groundwater flow, etc.), in many cases, tens to hundreds of years will typically be required to dissolve pools of CHC solvents in the saturated zone. Moreover, increased levels of effort (e.g., placement of additional wells, increased pumping, etc.) cannot be expected to shorten the time required for aquifer remediation by more than a factor of 5. Thus, for many sites contaminated with CHC solvents, remediation times will be unavoidably long. In those cases, the only cost-effective strategies may well be long term in nature (e.g., source containment and treatment combined with aqueous plume control) rather than the types of expensive, short-term "solutions" currently pursued.

Glossary

C	aqueous-phase concentration, g/m^3
C_{SAT}	saturation concentration, g/m^3
D_v	vertical dispersion coefficient, m^2/s
D_e	effective aqueous diffusion coefficient, m^2/s
F	surface-area-averaged flux from the aquitard, g m^{-2} day^{-1}
L_p	length of a pool in the direction of groundwater flow, m
M_a	surface-area-averaged mass-transfer rate, g m^{-2} day^{-1}
t	time
$\bar{v}$	average groundwater velocity, m/day
x	distance in the direction of groundwater flow, m
z	distance perpendicular to groundwater flow, m
α_v	vertical dispersivity, m
θ	porosity

ρ solvent density, g/m^3
τ_p time to complete pool dissolution, years

Registry No. TCE, 79-01-6.

Literature Cited

(1) Schwille, F. *Dense Chlorinated Solvents in Porous and Fractured Media—Model Experiments*, Translated by J. F. Pankow; Lewis Publishers: Boca Raton, FL, 1988.
(2) Anderson, M. R. Ph.D. Dissertation, Oregon Graduate Institute, 1988.
(3) Anderson, M. R.; Johnson, R. L.; Pankow, J. F. *Ground Water* **1992**, *30*, 250–256.
(4) Anderson, M. R.; Johnson, R. L.; Pankow, J. F. *Environ. Sci. Technol.* **1992**, *26*, following paper in this issue.
(5) Kueper, B. H. Ph.D. Dissertation, University of Waterloo, Waterloo, Ontario, 1989.
(6) Kueper, B. H.; Abbot, W.; Farquhar, G. *J. Contam. Hydrol.* **1989**, *5*, 83–95.
(7) Schmidtke, K.; McBean, E.; Rovers, F. In *Proceedings of the First National Outdoor Action Conference on Aquifer Restoration, Ground Water Monitoring, and Geophysical Methods*; 1987; pp 39–51.
(8) Freeze, R. A.; Cherry, J. A. *Groundwater*; Prentice-Hall: Englewood Cliffs, NJ, 1979.
(9) Hunt, J. R.; Sitar, M.; Udell, K. S. *Water Resour. Res.* **1988**, *24*, 1247–1259.
(10) Sudicky, E. A.; Cherry, J. A.; Frind, E. O. *J. Hydrol.* **1983**, *63*, 81–107.
(11) Sudicky, E. A. *Water Resour. Res.* **1986**, *22*, 2069–2082.
(12) Bird, R. B.; Stewart, W. E.; Lightfoot, E. N. *Transport Phenomena*; John Wiley and Sons: New York, 1960; p 541.
(13) Johnson, R. L.; Pankow, J. F.; Cherry, J. A. *Environ. Sci. Technol.* **1989**, *23*, 340–349.
(14) Crank. J. *The Mathematics of Diffusion*, 2nd ed.; Clarendon: Oxford, England, 1975; p 21.

Received for review October 25, 1991. Accepted December 9, 1991. This work was supported by the University Consortium Solvents-in-Groundwater Program with corporate support from Dow Chemical Corp., Ciba-Geigy Corp., General Electric Corp., Eastman Kodak Corp., and Boeing Corp.

Dissolution of Dense Chlorinated Solvents into Groundwater. 3. Modeling Contaminant Plumes from Fingers and Pools of Solvent

Michael R. Anderson,† Richard L. Johnson, and James F. Pankow*

Department of Environmental Science and Engineering, Oregon Graduate Institute, 19600 N. W. von Neumann Drive, Beaverton, Oregon 97006-1999

■ Chlorinated hydrocarbon (CHC) solvents are frequently observed groundwater contaminants. Groundwater concentrations of these compounds are generally below 1 mg/L, even at sites where it is known or at least strongly suspected that actual liquid CHC solvent is present in the saturated zone, and even though (1) these compounds are soluble at hundreds to thousands of milligrams per liter and (2) saturation is achieved relatively quickly when water flows through a porous medium containing droplets of CHC solvent. In this work, analytical transport models are used to examine why concentrations observed in the field are typically so low. The results suggest that the main reason is that CHC solvent below the water table tends to accumulate as stagnant pools located on the tops of low-permeability layers, or on top of an underlying aquitard. The rate at which CHC solvent dissolves from a pool into the flowing groundwater is controlled by vertical dispersion. Large fingers of solvent are not a likely source morphology in the saturated zone, and water flowing through many small fingers would cause such fingers to dissolve too quickly to be able to provide the type of long-term contamination that is observed at many CHC solvent spill sites.

Introduction

Accidental spills of chlorinated hydrocarbon (CHC) solvents are frequently very costly to remediate. In order to make the best groundwater remediation decisions, it is important to know as much as possible about the size and distribution of the source(s) of the subsurface contamination. The most common initial approach to source characterization is to analyze groundwater samples collected from monitoring wells. Unfortunately, groundwater-concentration data alone seldom provide adequate information. For example, the spatial variability usually observed in concentration data usually makes it very difficult to deduce the location(s) and size(s) of the source(s).

Although laboratory studies suggest that saturation is achieved relatively quickly when water flows through a porous medium containing some liquid solvent (*1*, *2*), (i.e., through a "finger" of solvent), the concentrations observed at solvent-contamination sites are usually *far* below saturation values. This remains true even in cases where it is known or at least strongly suspected that actual liquid CHC has reached the saturated zone. Thus, by itself, the observation of low CHC concentrations in groundwater cannot be used to argue against the presence of liquid CHC somewhere in the saturated zone.

Laboratory and theoretical studies suggest that, even in the most homogeneous of porous media, the infiltration of a dense CHC solvent into the saturated zone will be very erratic (*1*, *3*). In particular, when sufficient CHC head pressure exists to penetrate the water table, that penetration will tend to occur as a number of scattered "fingers" and not along one uniform plug or front. Kueper and Frind (*3*) have examined the fingering phenomenon from a theoretical perspective. Their analysis indicates that expected finger widths of common CHC solvents in sand or finer media should be less than 10 cm. Furthermore, their review of physical model experiments suggests that soon after the onset of finger formation, a small number of the fingers will grow at the expense of the others. This process and subsequent movement of the fingers will be controlled by heterogeneities within the formation.

No field-scale experiments have yet been reported which examine the penetration of CHC solvents in natural, heterogeneous media. Therefore, the sizes, shapes, and distributions of the CHC fingers that can develop in typical

†Present address: Oregon Department of Environmental Quality, Portland, OR.

0013-936X/92/0926-0901$03.00/0 © 1992 American Chemical Society

saturated zones following a large spill remain subject to considerable speculation. In the field, actual liquid CHC has been found in the saturated zone at only a few spill sites. At one such site, tri- and perchloroethylene (TCE and PCE) were found in an aquifer beneath an industrial facility (*4*). Although liquid-phase CHCs were found in wells over an irregularly shaped area measuring roughly 600 m by 600 m, neither the size(s) nor shape(s) of the CHC source zone(s) could be determined.

Erratic finger formation is not the only factor which complicates CHC solvent distribution in the saturated zone. Indeed, when a wandering, infiltrating finger of solvent encounters a low-permeability layer or lens, its downward movement can be stopped, and a shallow but extensive pool can form. What happens next in that region will depend on many factors. For a large release, the pool can grow to the extent that new fingers of solvent can be formed at the edges of the layer, and/or the pool may eventually develop sufficient head to penetrate into the layer. Thus, in any given case, the final subsurface distribution that results for a particular spill will be site-specific and unpredictable. Considering the unstable nature of immiscible finger flow, the subsurface distribution will not even be deterministic.

This paper utilizes modeling to determine the manner in which different fingers and pools of solvent will affect the characteristics of downgradient contaminant plumes. This will first be done in the context of three very simple source configurations (cases A, B, and AB). After the basic principles are illustrated, the distribution of contaminant from a more complicated source configuration will then be analyzed (case C). We will examine how the subsurface distributions of solvent might affect efforts to locate contamination sources, and how the natures of those sources (e.g., fingers vs pools) will affect source lifetimes.

Model Descriptions

General Procedures. Two analytical solutions to the three-dimensional advection–dispersion equation were used here. They were adapted from equations developed by Sudicky (*5*) for transport in an aquifer of finite thickness and infinite width. The use of analytical solutions required the making of certain simplifying assumptions, most importantly that the source regions examined have regular shapes and that the aquifer is homogeneous and isotropic. Sources involving multiple fingers or pools were handled by treating the overall source as a number of individual simple sources. The contribution from each part of the source was computed separately, and superposition was used to generate the overall contaminant distribution.

The assumptions regarding source regularity and aquifer homogeneity/isotropy were not considered overly restrictive since (1) the regularity of the source shape will decrease in importance with increasing distance from the source, (2) we have sought to investigate how the nature of CHC source zones will affect plume characteristics, but not to provide another study of how variable aquifer properties affect advective–dispersive transport, and (3) the distribution of fingers and pools will be controlled by aquifer heterogeneities; pools will tend to have dimensions which are smaller than the scale of heterogeneities within the aquifer, thus within the immediate vicinity of the CHC (i.e., where the dissolution process is occurring) the aquifer is probably relatively homogeneous.

Model 1. Plumes from Residual Fingers of CHC Solvent. To represent dissolution from a finger of solvent in a state of residual saturation, we assumed a vertical parallelepiped source configuration of square cross section

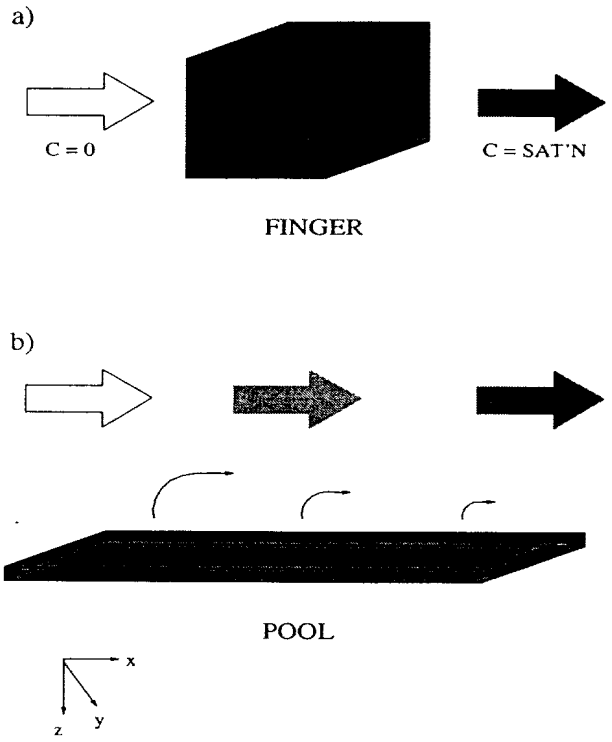


Figure 1. (a) Source geometry for eq 1; (b) source geometry for eq 4.

(Figure 1a). If there is no retardation, the analytical solution for the resulting contaminant plume is given by

$$C(x,y,z,t) = \frac{M_v}{4\theta}\int_0^t \left[\operatorname{erfc}\left(\frac{x-x_2-vt'}{2\sqrt{D_L t'}}\right) - \operatorname{erfc}\left(\frac{x-x_1-vt'}{2\sqrt{D_L t'}}\right)\right]\left[\operatorname{erfc}\left(\frac{y-y_0}{2\sqrt{D_h t'}}\right) - \operatorname{erfc}\left(\frac{y+y_0}{2\sqrt{D_h t'}}\right)\right]\left[\frac{z_2-z_1}{L} + \frac{2}{\pi}\sum_{k=1}^{\infty}\frac{1}{k}\cos\left(\frac{k\pi z}{L}\right)\times\left[\sin\left(\frac{k\pi z_2}{L}\right) - \sin\left(\frac{k\pi z_1}{L}\right)\right]\exp\left(\frac{-k^2\pi^2 D_v t'}{L^2}\right)\right] dt' \quad (1)$$

where the integral can be solved using Gaussian quadrature and the variables are defined as follows: $\bar{v}$, the mean groundwater velocity (L/T); θ, porosity; L, thickness of the aquifer (L); M_v, volumetric mass-transfer rate ($M/L^{-3}\,T^{-1}$); x_1, upstream x-coordinate of the source (L); x_2, downstream x-coordinate of the source (L); y_0, half-width of the source (L); z_1, upper z-coordinate of the source (from the top of the aquifer, L); z_2, lower z-coordinate of the source (from the top of the aquifer, L); D_L, coefficient of longitudinal dispersion (L^2/T); D_h, coefficient of horizontal transverse dispersion (L^2/T); and D_v, coefficient of vertical transverse dispersion (L^2/T). The three dispersion coefficients are given by

$$D_L = D_e + \alpha_L\bar{v} \qquad D_h = D_e + \alpha_h\bar{v} \qquad D_v = D_e + \alpha_v\bar{v} \quad (2)$$

where the variables are defined as follows: α_L, longitudinal dispersivity; α_h, transverse horizontal dispersivity; α_v, transverse vertical dispersivity; and D_e, effective molecular diffusion coefficient in the porous medium.

At steady state, the shape of a plume will not be affected by changes in α_L (i.e., by changes in dispersivity in the direction of flow). Changes in the transverse dispersivity α_v will affect the steady-state plume when the source does

not extend uniformly in the z-direction. An example of a source that is uniform in the z-direction would be a finger of constant width that extends from the top to the bottom of the aquifer. The solution represented by eq 1 arbitrarily assumes that the manner in which the concentration of the water flowing through the finger approaches saturation is linear with distance through the finger. The rate of approach to saturation is set by the value of M_v. There is good evidence that water moving at typical groundwater velocities through virtually any finger larger than a few centimeters will leave the finger saturated at the equilibrium solubility C_{SAT} (2). Thus, in order to produce saturated concentrations in the flow from any given finger, for each finger we adjusted M_v according to

$$M_v = C_{SAT}\theta\bar{v}/(x_2 - x_1) \quad (3)$$

The flow occurs in the positive x-direction. The quantity $(x_2 - x_1)$ is the dimension of the finger in the direction of flow. For the illustrations considered here, the value of C_{SAT} was set equal to 200 mg/L, the aqueous solubility of PCE at 20 °C. Equations 1 and 3 assume that horizontal transverse dispersion dissolves only negligible solvent from the two xz-sides of the finger. At a water velocity of 30 cm/day and with a microscale (grain-size scale) horizontal transverse dispersivity of $\alpha_h = \sim 0.0003$ m/day [representative of transverse dispersion values observed in the laboratory (1)], this assumption is valid for fingers with widths larger than a few centimeters. The assumption becomes increasingly valid as the finger dimension increases because the flow out of the yz-face of the finger is always saturated, and so the mass flow increases linearly with the width. The net diffusive mass transport from the xz-faces of the finger, however, does not increase linearly with the size of the finger.

All solvent fingers were assumed to be centered on and along the line $x = 0$, i.e., along the y-axis. In a real spill, infiltration may occur all around the spill origin, at points with both positive and negative x-values. Centering all fingers on the y-axis is adequate because (1) the transport delay affecting the portions of a source with $x < 0$ will be partially counterbalanced by the head start of the portions with $x > 0$ and (2) at long travel distances from the source region, small differences in the x-coordinates of the source distribution will not have a significant effect on the resulting contaminant distribution.

Model 2. Plumes from Pools of CHC Solvent. The rate of dissolution into groundwater flowing above a thin pool of CHC will be controlled by the rate at which vertical dispersion can move the contaminant away from the pool/water interface and into the clean water above the pool. Since pools will tend to form on the tops of less-permeable layers, we will assume that pools lose significant mass only into the groundwater that is *above* the pool.

As discussed in detail by Johnson and Pankow (6), the amount of mass that will move into the groundwater above a given pool will depend on C_{SAT}, α_v, D_e, $\bar{v}$, and the residence time of the groundwater above the pool. The value of C_{SAT} is important because the water directly at the pool/water interface will be saturated. This saturation value sets one of the boundary conditions for dispersion upward and away from the pool. In a semi-infinite medium, the other boundary condition will be $C(x,y,z = \infty, t = \infty) = 0$.

If the shape of the pool can be approximated as a square, the residence time above the pool will be given by the length of the pool $(x_2 - x_1) = L_p$ in the direction of the flow divided by the mean groundwater velocity $\bar{v}$. Neglecting the effects of concentration gradients in the x-direction, the amount of solvent that will dissolve into a parcel of water moving above a pool will be approximately the same as if the parcel was stationary and was exposed to the pool for a time period equal to the residence time above the pool.

The equation for the *surface-area-averaged* mass-transfer rate (M_a) is (6)

$$M_a = C_{SAT}\theta\sqrt{4D_v\bar{v}/\pi L_p} \quad (4)$$

The only laboratory data for the dissolution of CHC solvent pools is that of Schwille (7) for TCE dissolving into medium-grained sand. On the basis of that data, Johnson and Pankow (6) report a value of ~0.000 23 m/day for α_v. Using that value, with groundwater moving at 30 cm/day above PCE pools, the approach of Johnson and Pankow (6) yields M_a values of 0.32, 0.26, 0.22, and 0.12 g m^{-2} day^{-1} for pools with lengths of 2, 3, 4, and 10 m, respectively.

The trend of decreasing M_a with increasing pool length may be understood as follows. The residence time above the pool and the overall rate of dissolution in units of grams per day will increase as the length of the pool in the direction of the flow increases. However, as the water moves across the top of the pool, the concentration gradient at the water/pool interface decreases, and so the instantaneous dissolution rate also decreases. Thus, since we express the pool mass-transfer rate as M_a in units of grams per square meter per day, the value of M_a decreases as the length of the pool increases.

The value of M_a for a pool of given dimensions can be used as an input parameter for the transport model. For reasons similar to those discussed for solvent fingers, all solvent pools were assumed to have square cross sections centered on the y-axis. The thickness of a pool was assumed to be insignificant relative to the thickness of the aquifer. Therefore, only the depth of the pool from the top of the aquifer (z_0) was necessary to define the location of a pool. It was assumed that the retardation is zero. By use of Gaussian quadrature to solve the integral expression, the contaminant distribution resulting from the dissolution of the thin, square pools (Figure 1b) was simulated using

$$C(x,y,z,t) = \frac{M_a}{4\theta L}\int_0^t \left[\operatorname{erfc}\left(\frac{x - x_2 - vt'}{2\sqrt{D_L t'}}\right) - \operatorname{erfc}\left(\frac{x - x_1 - vt'}{2\sqrt{D_L t'}}\right)\right]\left[\operatorname{erfc}\left(\frac{y - y_0}{2\sqrt{D_h t'}}\right) - \operatorname{erfc}\left(\frac{y + y_0}{2\sqrt{D_h t'}}\right)\right]\left[1 + 2\sum_{k=1}^{\infty}\cos\left(\frac{k\pi z}{L}\right)\cos\left(\frac{k\pi z_0}{L}\right)\times \exp\left(\frac{-k^2\pi^2 D_v t'}{L^2}\right)\right] dt' \quad (5)$$

Hypothetical CHC Spills

It was assumed for each spill modeled that liquid PCE entered a 15-m-thick saturated zone underlain by an impermeable layer. The porosity and mean water velocity in the aquifer were assumed to be 0.35 and 30 cm/day, respectively. PCE in a finger was assumed to be present as an immobile residual. The residual saturation in each finger (percent of the void volume occupied by the solvent) was assumed to be 15%. Thus, 52.5 L of PCE was assumed present in each cubic meter of aquifer that contained PCE at residual saturation. Volatilization losses to the vadose zone were not considered.

Simple Finger and Pool Source Configurations. In case A, a single 20 × 20 cm finger of PCE was assumed to be present in the aquifer. With a total height of 15 m, the

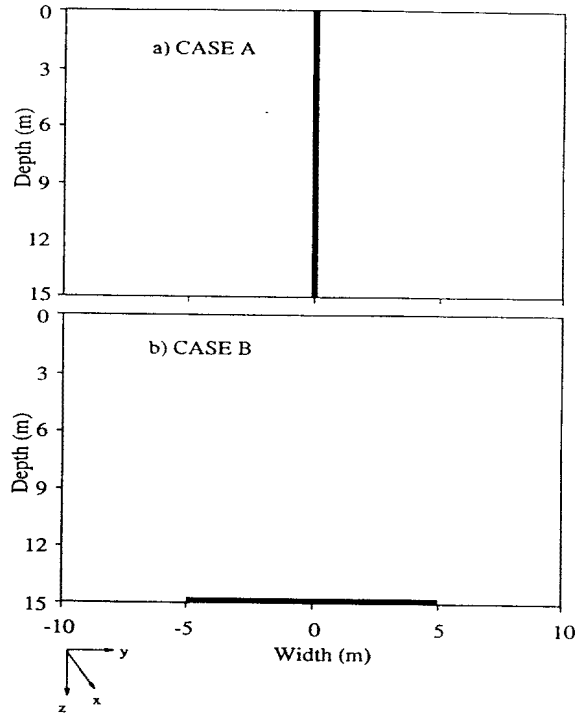


Figure 2. (a) Source geometry for case A, finger dimensions are 0.2 m by 0.2 m by 15 m tall; (b) source geometry for case B, pool dimensions are 10 m by 10 m.

finger occupied 0.60 m^3 of the aquifer and contained 31.5 L of PCE (Figure 2a). By most standards, a spill of 31.5 L is a small spill. For case B, 968.5 L was taken as the spill volume with the solvent spread over a pool that was 10 × 10 m (Figure 2b). For case AB, the spill volume was taken to be 1000 L, with 31.5 L present in a finger like that in case A, and 968.5 L in a pool like that in case B. The downgradient concentration values for case AB were obtained by summing the values produced by Model 1 for case A and model 2 for case B.

Multiple Fingers and Pools. Because a dense CHC solvent will tend to split into multiple fingers and pools as it moves downward into the saturated zone, a simulation was conducted to investigate the contaminant plume from a source consisting of multiple fingers and multiple pools. Case C thus represents a solvent spill that penetrated the water table in one location, then split into various fingers and pools as it made its way toward the bottom of the aquifer. The vertical bars in Figure 3 represent the locations of the fingers. The horizontal bars represent pools where the CHC solvent encountered a zone of slightly lower permeability and therefore spread out until it could move downward again. The widths of the fingers were assumed to decrease with increasing depth, starting with a width of 10 cm for the first finger and ending with a width of 2 cm for the lowest fingers. As in cases A and B, all fingers and pools were assumed to have square horizontal cross sections. The dimensions of the 12 pools ranged from 2 to 4 m. The average dimension was chosen to be 3 m, which is typical of the scales of horizontal layers in aquifers (*8*).

The x-, y-, and z-limits and the PCE volumes for the various fingers and pools in case C are summarized in Table I for this ~1000-L spill. The values in Table I give a total of ~7 L for the volume of PCE in the fingers, and 983 L for the pools. The numbers of fingers and pools represented in Figure 3 may be conservative, particularly with regard to the number of fingers. Nevertheless, for many spill sites it is likely that the bulk of the CHC solvent will end up in pools rather than fingers.

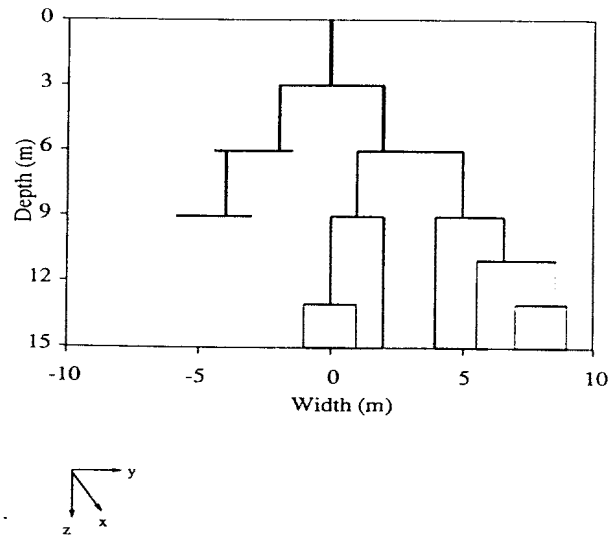


Figure 3. Source geometry for case C. Specific locations and dimensions of the fingers and pools are listed in Table I.

Table I. Lengths, Widths, and Heights (in Meters) of the Fingers and Pools Used in Case C

Fingers

	x_1	x_2	y_1	y_2	z_1	z_2	solvent vol,[a] L	lifetime, years
1	−0.05	0.05	−0.05	0.05	0.0	3.0	1.58	1.1
2	−0.04	0.04	−2.04	−1.96	3.0	6.0	1.01	0.9
3	−0.04	0.04	1.96	2.04	3.0	6.0	1.01	0.9
4	−0.03	0.03	−4.03	−3.97	6.0	9.0	0.57	0.7
5	−0.03	0.03	0.97	1.03	6.0	9.0	0.57	0.7
6	−0.03	0.03	4.97	5.03	6.0	9.0	0.57	0.7
7	−0.02	0.02	−0.02	0.02	9.0	13.0	0.34	0.4
8	−0.02	0.02	1.98	2.02	9.0	15.0	0.50	0.4
9	−0.02	0.02	3.98	4.02	9.0	15.0	0.50	0.4
10	−0.02	0.02	6.48	6.52	9.0	11.0	0.17	0.4
11	−0.01	0.01	5.49	5.51	11.0	15.0	0.08	0.2
12	−0.01	0.01	8.49	8.51	11.0	13.0	0.04	0.2
13	−0.01	0.01	−1.01	−0.99	13.0	15.0	0.04	0.2
14	−0.01	0.01	0.99	1.01	13.0	15.0	0.04	0.2
15	−0.01	0.01	6.99	7.01	13.0	15.0	0.04	0.2
16	−0.01	0.01	8.99	9.01	13.0	15.0	0.04	0.2
total							7.10	

Pools

	x_1	x_2	y_1	y_2	z	solvent vol, L	lifetime, years
1	−2.00	2.0	−2.0	2.0	3.0	224	273
2	−1.50	1.5	−4.5	1.5	6.0	95	177
3	−2.00	2.0	1.0	5.0	6.0	224	273
4	−2.00	2.0	−4.5	−3.0	9.0	55	134
5	−1.00	1.0	0.0	2.0	3.0	28	96
6	−1.50	1.5	4.0	6.5	9.0	55	134
7	−1.50	1.5	5.5	8.5	11.0	95	177
8	−1.00	1.0	−1.0	1.0	13.0	28	96
9	−1.00	1.0	7.0	9.0	13.0	28	96
10	−2.00	2.0	−1.0	2.0	15.0	95	177
11	−1.00	1.0	4.0	6.0	15.0	28	96
15	−1.50	1.5	7.0	9.0	15.0	28	96
total						983	

[a] Calculated by assuming the liquid PCE occupied 15% of the total pore space.

Results and Discussion

Cases A, B, and AB. Steady-state concentration contours were obtained for cases A, B, and AB using $\alpha_L = 1$ m, $\alpha_h = 0.1$ m, $\alpha_v = 0.000\,23$ m, and $D_e = 4.3 \times 10^{-10}$ m^2/s. Although the value of α_L will not affect the concentration

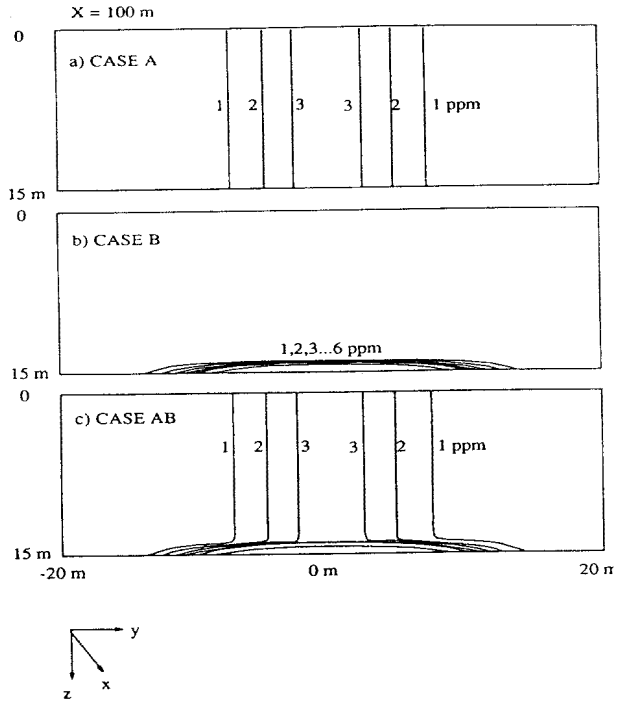


Figure 4. Concentration contours in the plane perpendicular to the groundwater flow (*yz*-plane) at 100 m downgradient from the source. (a) Case A; (b) case B; (c) case AB. Contour intervals are 1, 2, 3, 4, 5, and 6 ppm.

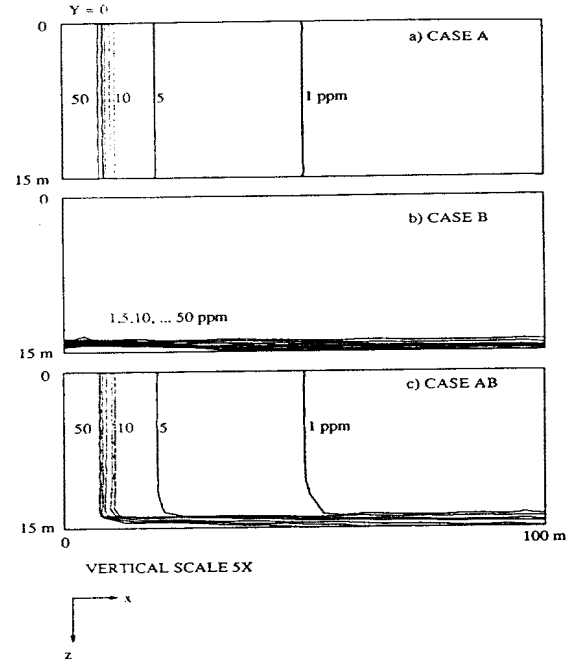


Figure 5. Concentration contours in the vertical section through the center of the source (*xz*-plane) in the direction of groundwater flow. (a) Case A; (b) case B; (c) case AB. Contour intervals are 1, 5, 10, 20, 30, 40, and 50 ppm.

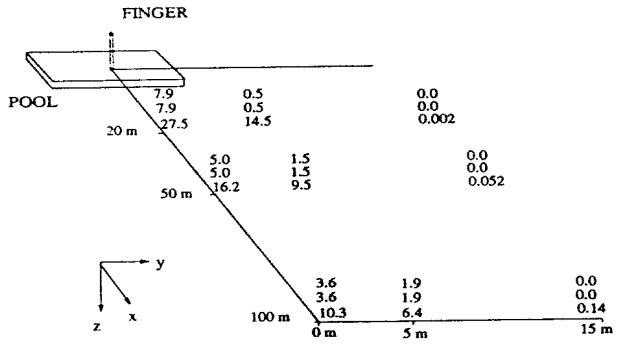


Figure 6. Simulated well data (ppm) for 2-m screened intervals at depths of 0–2, 6.5–8.5, and 13–15 m for case AB.

characteristics of any of the steady-state plumes, a specific value was needed as an input to the models in order to obtain the steady-state distributions at long time. The relatively small value for α_v was selected based on the observation by Sudicky (*8*) and others that vertical spreading at the field scale in sandy aquifers can be governed by dispersion occurring at the grain-size scale.

The steady-state results for the *yz* cross sections at 100 m downgradient (x = 100 m) are presented for cases A, B, and AB in Figure 4a–c. For the uniform vertical source in case A, α_h is the only dispersivity that affects the steady-state distribution. An α_h value of 0.1 m is on the low end of the range that has traditionally been considered typical at the field scale (*9*). Figure 4a should therefore be a lower bound for the degree of spreading (i.e., dilution) taking place in the contaminant plume for this spill. The concentration in the center of the plume at x = 100 m is 3.4 ppm at all depths.

For the case B simulation, the PCE is present as a single 10 × 10 m pool. For this case, the values of both α_h and α_v will affect the steady-state distribution of contaminant. Unlike case A, this source configuration is not uniform in depth. Thus, the downgradient contaminant distribution is depth-dependent. As illustrated in Figure 4b, at x = 100 m, the contaminant levels increase rapidly toward the bottom of the aquifer. At 1 m from the bottom of the aquifer, the concentration is 0.1 mg/L, and at the bottom the concentration maximizes at ~20 mg/L. Figure 4c provides the contours for case AB. In the upper portion of the aquifer, the contours are indistinguishable from those for case A. Near the bottom, the contours are indistinguishable from those for case B. Figure 5 presents concentration contours for the three cases on an *xz*-plane through y = 0.

Although contour plots such as those discussed above provide good visual representations of the sizes and shapes of the modeled plumes, it is important to recognize that the level of contamination that will be encountered in a sampling well will be an *average* that is determined by the screened interval of the well. To illustrate this, nine well nests were assumed to be present in the case AB zone of contamination. Three nests were located on the center line (y = 0) of the plume at distances of x = 20, 50, and 100 m downgradient from the spill origin. Three more nests were located at the same x-distances, but were offset at y = 5 m from the center line. The final three nests were offset at y = 15 m from the centerline. Each nest was assumed to have three monitoring wells, the screened interval of each was taken to be 2 m long. For each nest, the three wells were considered to be screened from z = 0 to 2 m, z = 6.5 to 8.5 m, and z = 13 to 15 m.

The water sampled from each of the intervals was assumed to contain a contaminant concentration equal to the volume-averaged value over the screened interval. Figure 6 presents the concentrations that would be found at steady state in each of the 27 monitoring wells for case AB. In the upper portion of the aquifer, contamination from the case A portion of the source dominates; in the lower portion of the aquifer, contamination from the case B portion of the source dominates. At a y-offset of 5 m from the center line, the concentrations are 1.5 mg/L at x = 50 m and 1.9 mg/L at x = 100 m. These results indicate how horizontal transverse dispersion can cause the concentration to increase (at least initially) with dis-

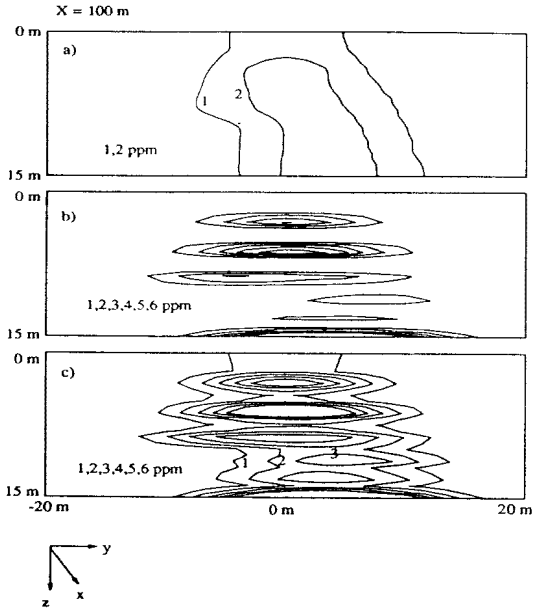


Figure 7. Concentration contours in the plane perpendicular to the groundwater flow (yz-plane) at 100 m downgradient from the source for case C. (a) Fingers only; (b) pools only; (c) fingers and pools. Contour intervals are 1, 2 , 3, 4, and 5 ppm.

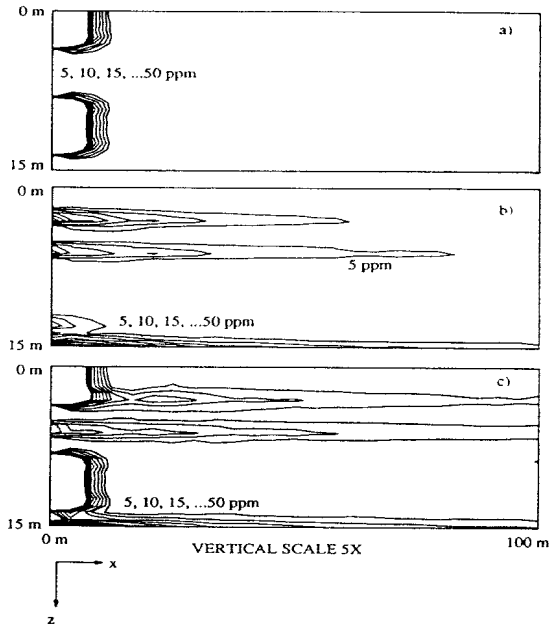


Figure 8. Concentration contours in the vertical section (y = 0 in xz-plane) in the direction of groundwater flow for case C. (a) Fingers only; (b) pools only; (c) fingers and pools. Contour intervals are 5, 10, 15, 20, 25, 30, 35, 40, 45, and 50 ppm.

tance *away* from the source along a transect that is offset from the plume centerline.

More importantly, we note that the contaminant concentrations in the upper portion of the aquifer are only a few milligrams per liter at x = 20 m. At a y-offset of just 15 m from the center line, the concentrations are only 0.0, 0.0, and 0.055 mg/L at 50 m downgradient. Thus, the important point here is that even in cases where substantial amounts of liquid PCE have been spilled and are still present in the aquifer as a pool, the concentrations found relatively close to the source can be far below saturation. This is consistent with observations at actual spill sites.

Case C. The dispersivity values used for case C were the same as those for the other cases. Figure 7 presents the steady-state PCE concentrations for case C for the yz cross section at x = 100 m. The complex nature of the source leads to a downgradient contaminant distribution that is dependent on depth and is not symmetric around the x-axis. The maximum concentration of ~10 mg/L at the bottom right portion of the aquifer is a result of the three pools located there. Figure 8 presents the contours for the xz cross section at y = 0. For each figure, part a contains the fingers-only contributions, part b contains the pools-only contribution, and part c contains the sum of both contributions.

The relative contributions to the steady-state contamination from the fingers and from the pools can be obtained by areally integrating the masses under the contours in Figure 7, parts a and b, respectively. The results are 0.5 and 0.4 kg/m, respectively. (The units for these values correspond to mass per unit thickness of aquifer in the direction of flow.) Thus, in this example, where the number of fingers was relatively small, the assemblage of fingers and the assemblage of pools contribute about equally to the steady-state contamination distribution, at least initially. Simulated well data for case C is presented in Figure 9. As was observed for case AB, even with a large spill volume, the concentrations found in much of the aquifer can be far below saturation.

Relative Lifetimes of Fingers and Pools. Although some of the concentrations discussed above may be very

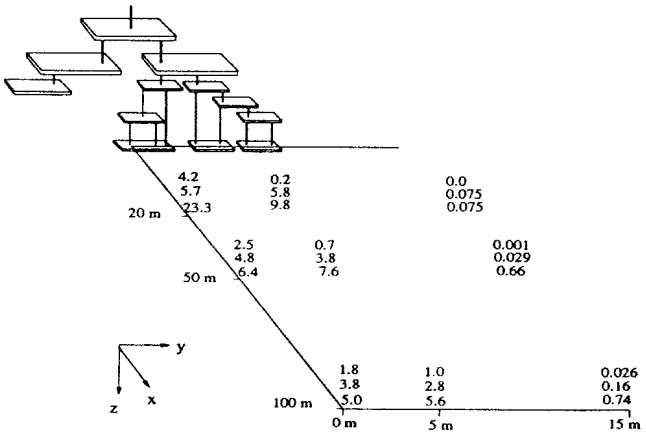


Figure 9. Simulated well data (ppm) for 2-m screened intervals at depths of 0–2, 6.5–8.5, and 13–15 m for case C.

high relative to current drinking water standards, they are still low on an absolute scale. Thus, when a significant volume of liquid CHC solvent is present as a source, the lifetime of that source can be very large (e.g., hundreds of years) relative to desired remediation times.

Since it was assumed that all water flowing through a residual finger becomes saturated with solvent, a lower limit of the time for total dissolution of a finger (τ_f) can be calculated from

$$\tau_f = m_f / V_f M_v \qquad (6)$$

where m_f is the total mass of residual solvent in the finger and V_f is the volume of the finger.

A lower limit of the time for total removal of a pool (τ_p) can be calculated from

$$\tau_p = m_p / A_p M_a \qquad (7)$$

where m_p is the mass of solvent in the pool and A_p is the initial surface area of the pool. Removal times calculated using eqs 6 and 7 are only lower limits since the total dissolution rates will slow as the fingers and pools dissolve. Indeed, as the removal proceeds, the cross-sectional area of a finger perpendicular to the groundwater flow may

decrease due to preferential flow around rather than through the finger. However, the magnitude of the effect is likely to be small for typical values of residual saturation (2, 3). For a pool of uniform thickness, the upgradient portion will definitely dissolve away before the downgradient portion, thus leading to a decrease in pool area with time. Nevertheless, as discussed by Johnson and Pankow (6), eq 7 still provides a reasonable estimate of τ_p.

Even though the width of the single finger considered in case A (i.e., 10 cm) is on the upper end of the range expected for porous media, the removal time calculated using eq 6 is relatively short (~2 years). For the pool in case B, eq 7 gives ~1000 years as the lower estimate of the lifetime. Thus, for the finger/pool combination considered in case AB, after about 2 years, there is no doubt that the contamination distribution would take on the character of the case B source for a very long period of time.

The lower estimates of the lifetimes of the multiple fingers and pools making up the case C source are collected in Table I. As with case AB, we see that it is the pools rather than the fingers that will serve as long-term sources in the system. The values in Table I can be compared with the initial integrated finger and pool contributions of 0.5 and 0.4 kg/m calculated from Figure 7, panels a and b. For a groundwater velocity of 0.3 m/day and a porosity of 0.35, these integrated contributions lead to initial overall finger and pool dissolution rates of 0.052 and 0.042 kg/day, respectively. Those rates, along with the total volumes originally in the fingers and pools (7 and 983 L, respectively), provide estimates of the average dissolution times for the fingers and pools of ~1 and 100 years, respectively. The individual estimates of the lifetimes are given in Table I.

As mentioned previously, the fact that the individual fingers are small means that their lifetimes will be short (e.g., a few years) at sites where there is significant groundwater flow (e.g., >0.1 m/day). Thus, at such sites, where spills are several years old, all of the fingers are likely to have dissolved away, with all of the observed dissolved contaminant coming from the pools. Overall, we see that (1) CHC solvent in the saturated zone can cause very long term contamination and that (2) a long-lived source is quite possibly a pool. [Another possible long-lived source is a low-permeability zone that has been exposed to a pool for a significant amount of time (6)].

In investigations of groundwater contamination problems resulting from immiscible solvent spills, the number of sampling wells that are installed are frequently limited by financial considerations. It is also true that the number of wells is almost always less than that desired by those responsible for analyzing the data and planning the remedial action. However, the sampling results for the hypothetical spills discussed above make an important point about the strategy of spill investigations. That is, information gathered at several discrete depths within a given well by means of a true multilevel sampling device may be just as or more important than information gathered from horizontally-resolved wells. In cases where significant differences exist in the permeability of adjacent water-bearing zones, depth-resolved wells have been shown to improve not only the reliability of contaminant-level data, but also the hydrologic data (10). Therefore, installation of depth-resolved sampling devices should certainly always be considered as a possible option for improving site investigation results.

Conclusions

Model studies of the type presented here provide insight into the nature of the contamination which results from different types of liquid CHC sources in the saturated zone. These insights can be examined in the context of the fact that groundwater concentrations at sites where significant liquid CHC solvent has been spilled are typically very low relative to saturation. One probable reason for this is that the cross-sectional area of the source when viewed from upgradient may be only a few percent of the total vertical cross-sectional area of the aquifer. As a consequence, dispersion of the dissolved CHC will lead to substantial dilution.

As the examples presented here demonstrate, CHC concentration distributions in the groundwater zone can be highly spatially variable. In addition to dispersion, vertically-averaged sampling from conventional monitoring wells can lead to observed concentrations which are substantially below the maximum values present in the aquifer. Unless caution is observed when those averaged results are being interpreted, incorrect conclusions about the distribution of CHC in the subsurface may be drawn.

We also believe that, in many cases, most of the mass of the CHC will be in pools rather than in fingers, and that dissolution will occur more readily from the fingers than from the pools. These two conclusions suggest that the fingers may be relatively short-lived, and that for most of the time required for CHC dissolution, aqueous concentrations will be determined by dissolution from pools.

Glossary

A_p	initial surface area of a pool
C	aqueous-phase concentration, g/m^3
C_{SAT}	saturation concentration, g/m^3
D_e	effective aqueous diffusion coefficient, m^2/s
D_L	coefficient of longitudinal dispersion, m^2/s
D_h	coefficient of horizontal transverse dispersion, m^2/s
D_v	coefficient of vertical transverse dispersion, m^2/s
L	thickness of the aquifer, m
L_p	length of a pool in the direction of groundwater flow, m
M_a	surface-area-averaged mass-transfer rate, g m^{-2} s^{-1}
M_f	mass of a solvent in a finger, g
M_p	mass of a solvent in a pool, g
M_v	volumetric mass-transfer rate, g m^{-3} s^{-1}
t	time
$\bar{v}$	average groundwater velocity, m/day
V_f	volume of a finger, m^3
x	distance in the direction of groundwater flow, m
x_1	upstream coordinate of the source, m
x_2	downstream coordinate of the source, m
y_0	half-width of the source, m
z_0	depth of the pool from the top of the aquifer, m
z_1	upper z-coordinate of the source, m
z_2	lower z-coordinate of the source, m
α_h	transverse horizontal dispersivity, m
α_L	longitudinal dispersivity, m
α_v	vertical dispersivity, m
θ	porosity
ρ	solvent density, g/m^3
τ_f	time to complete finger dissolution, years
τ_p	time to complete pool dissolution, years

Registry No. PCE, 127-18-4.

Literature Cited

(1) Anderson, M. R. Ph.D. Dissertation, Oregon Graduate Institute, 1988.

(2) Anderson, M. R.; Johnson, R. L.; Pankow, J. F. *Ground Water* **1992**, *30*, 250–256.

(3) Kueper, B. H.; Frind, E. O. *J. Contam. Hydrol.* **1988**, *2*, 95–110.

(4) Schmidtke, K.; McBean, E.; Rovers, F. In *Proceedings of the First National Outdoor Action Conference on Aquifer Restoration, Ground Water Monitoring and Geophysical Methods*; 1987; pp 39–51.

(5) Sudicky, E. A. University of Waterloo, Waterloo, Ontario, Canada, personal communication to Michael R. Anderson of the Oregon Graduate Institute, 1988.
(6) Johnson, R. L.; Pankow, J. F. *Environ. Sci. Technol.*, preceding paper in this issue.
(7) Schwille, F. *Dense Chlorinated Solvents in Porous and Fractured Media*, Translated by J. F. Pankow; Lewis Publishers: Boca Raton, FL, 1988.
(8) Sudicky, E. A. *Water Resour. Res.* **1986**, *22*, 2069–2082.
(9) Anderson, M. P. *CRC Crit. Rev. Environ. Control* **1979**, *9*, 97–156.
(10) McIlvride, W. A.; Rector, B. M. In *Proceedings of the Second National Outdoor Action Conference on Aquifer Restoration, Ground Water Monitoring and Geophysical Methods*; 1988; pp 375–390.

Received for review October 25, 1991. Accepted December 9, 1991. This work was supported by the University Consortium Solvents-in-Groundwater Program with corporate support from Dow Chemical Corp., Ciba-Geigy Corp., General Electric Corp., Eastman Kodak Corp., and Boeing Corp.

points to a role as

 0013-936X/92/0926-0908$03.00/0 © 1992 American Chemical Society